Biochemical and Biophysical Research Communications 415 (2011) 17–23

Contents lists available at SciVerse ScienceDirect

Biochemical and Biophysical Research Communications

journal homepage: www.elsevier.com/locate/ybbrc

Inverted repeats in the promoter as an autoregulatory sequence for TcrX in *Mycobacterium tuberculosis*

Monolekha Bhattacharya, Amit Kumar Das *

Department of Biotechnology, Indian Institute of Technology Kharagpur, Kharagpur 721302, India

ARTICLE INFO

Article history:
Received 23 September 2011
Available online 6 October 2011

Keywords:
Response regulator
TcrX
Crosslinking
Protein–DNA docking
EMSA

ABSTRACT

TcrY, a histidine kinase, and TcrX, a response regulator, constitute a two-component system in *Mycobacterium tuberculosis*. *tcrX*, which is expressed during iron scarcity, is instrumental in the survival of iron-dependent *M. tuberculosis*. However, the regulator of *tcrX/Y* has not been fully characterized. Crosslinking studies of TcrX reveal that it can form oligomers *in vitro*. Electrophoretic mobility shift assays (EMSAs) show that TcrX recognizes two regions in the promoter that are comprised of inverted repeats separated by ~30 bp. The dimeric *in silico* model of TcrX predicts binding to one of these inverted repeat regions. Site-directed mutagenesis and radioactive phosphorylation indicate that D54 of TcrX is phosphorylated by H256 of TcrY. However, phosphorylated and unphosphorylated TcrX bind the regulatory sequence with equal efficiency, which was shown with an EMSA using the D54A TcrX mutant.

1. Introduction

Two-component systems (TCSs) consisting of a histidine kinase (HK) and a response regulator (RR) are responsible for the ability of a pathogen to adapt to a hostile host environment [1]. In response to a specific signal, the HK sensor is autophosphorylated at a conserved histidine residue in an ATP-dependent manner. The phosphoryl group is then transferred to a conserved aspartate residue in the RR, which leads to an altered ability to bind target DNA and activate gene expression [2]. The genes for a HK and its cognate RR are typically transcribed from a single operon [1]. In *Mycobacterium tuberculosis*, the genome contains twelve paired TCS genes, two orphan HK genes, and five orphan RR genes. Mycobacterial TCS RRs correspond to 0.6% of the total genes; a similar abundance to that observed in *Corynebacterium diphtheriae*, *Bacillus subtilis*, and *Escherichia coli* [3]. Among mycobacterial RRs, PhoP positively regulates complex lipid biosynthesis in Mycobacteria, *mprA* is required for persistent lung infection, and *devR–devS* is induced under hypoxic conditions [4–6]. Considering the importance of mycobacterial RRs toward the virulence of a pathogen, insight into the HK-RR and subsequent RR-DNA interaction sites in *M. tuberculosis* would aid in structure-based inhibitor design.

The interacting TCS pair conserved in all species of Mycobacteria except *Mycobacterium leprae* [7] is RR (TcrX) and HK (TcrY) encoded by the two adjacent ORFs Rv3765c and Rv3764c, respectively. The gene *tcrX* is overexpressed under conditions of limited iron [8] and during the growth periods in macrophages [9]. Because *M. tuberculosis* is dependent on iron for survival, the expression of *tcrX* in iron depletion conditions highlights the importance of this RR in tuberculosis. In a severe combined immunodeficient (SCID) mouse model, deletion of *tcrX/Y* from mycobacteria increased virulence, with significantly shorter survival times for the mice [10]. The TcrX/Y system has been shown to be a true TCS with the commonly conserved residues TcrY/H256 and TcrX/D54/D59 [11]. TcrX belongs to the OmpR/PhoB subfamily, which is characterized by a winged helix-turn-helix domain [12,13]. Representative RR families other than OmpR/PhoB are NarL/FixJ [14,15] and NtrC/DctD [16]. It is essential to identify the regulatory sequence in the promoter to understand the autoregulation of TcrX.

Here, an attempt is made to identify the TcrX regulatory sequence in the promoter, the oligomerization state of TcrX, the active sites of phosphorylation of TcrX/Y and the kinetics of phosphorylation.

2. Materials and methods

2.1. Cloning, overexpression and purification of TcrX/Y

Full-length TcrX (residues 1–234) and a truncated TcrY construct (residues 241–475) were used to obtain the recombinant protein in the cytosolic fraction because the full length TcrY was insoluble. TcrX and TcrY were purified as described elsewhere [11], and the conserved residues were mutated. Mutants *tcrY* (H256Q) and *tcrX* (D54A/D59A) were amplified [17] using gene specific primers (Supplementary Table 1) and cloned into pGEX4T3 and pQE30 expression vectors, respectively. Truncated TcrY (H256Q) was purified by GST affinity chromatography and dialyzed against

* Corresponding author. Fax: +91 3222 255303.
E-mail address: amitk@hijli.iitkgp.ernet.in (A.K. Das).

0006-291X/$ - see front matter © 2011 Elsevier Inc. All rights reserved.
doi:10.1016/j.bbrc.2011.09.143

buffer containing 50 mM Tris–HCl, pH 8.0 and 2 mM DTT. Full-length TcrX (D54A/D59A) was purified to homogeneity using Ni-NTA chromatography and dialyzed against buffer containing 20 mM Tris–HCl, pH 8.0, 300 mM NaCl and 2 mM DTT.

2.2. Phosphorylation assays

Autophosphorylation was performed with 15 μM TcrY (wild-type or H256Q) in a volume of 20 μl for 2 h in the presence of 10 μCi [γ-^{32}P] ATP and unlabeled ATP [11] followed by addition of 15 μM TcrX (wild type or D54A/D59A) after which the reaction was continued for 7 h at 25 °C to allow for phosphotransfer. The quenched reactions were subjected to 15% SDS–PAGE followed by autoradiography and TcrY bands were excised from the stained 15% SDS–PAGE gels for treatment with CocktailW (SRL, India). The disintegration counts were measured in a liquid scintillation analyzer from Perkin Elmer (Fig. S1C). For phosphotransfer kinetics, the autophosphorylation reaction mixture was first incubated in the presence of 10 μCi [γ-^{32}P] ATP for 6 h at 25 °C for maximum incorporation of ^{32}P into TcrY. TcrX (15 μM) was then added to varying concentrations of phosphorylated TcrY (P-TcrY), and the reaction was continued for an additional 6 hrs. The bands of TcrX from stained gels of 15% SDS–PAGE were treated with CocktailW (SRL, India), for measurement of disintegration counts in a liquid scintillation analyzer. The initial velocities of ^{32}P incorporation into TcrX for different P-TcrY concentrations from three independent experiments were fit with the Michaelis–Menten equation:

$$v = \frac{V_{\max}[S]}{K_m + [S]} \tag{1}$$

where v is the initial velocity, $V_{\max}$ is the maximum reaction velocity, $[S]$ is the substrate concentration and K_m is the Michaelis–Menten constant. K_m was determined from a Lineweaver–Burk plot using the following equation:

$$\frac{1}{v} = \frac{1}{V_{\max}} + \frac{K_m}{V_{\max}} \times \frac{1}{[S]} \tag{2}$$

2.3. Crosslinking of TcrX

Phosphorylated TcrX (P-TcrX) was prepared by incubating TcrX in a reaction mixture of 10 μCi [γ-^{32}P] ATP (>3300 Ci/mmol, BRIT,

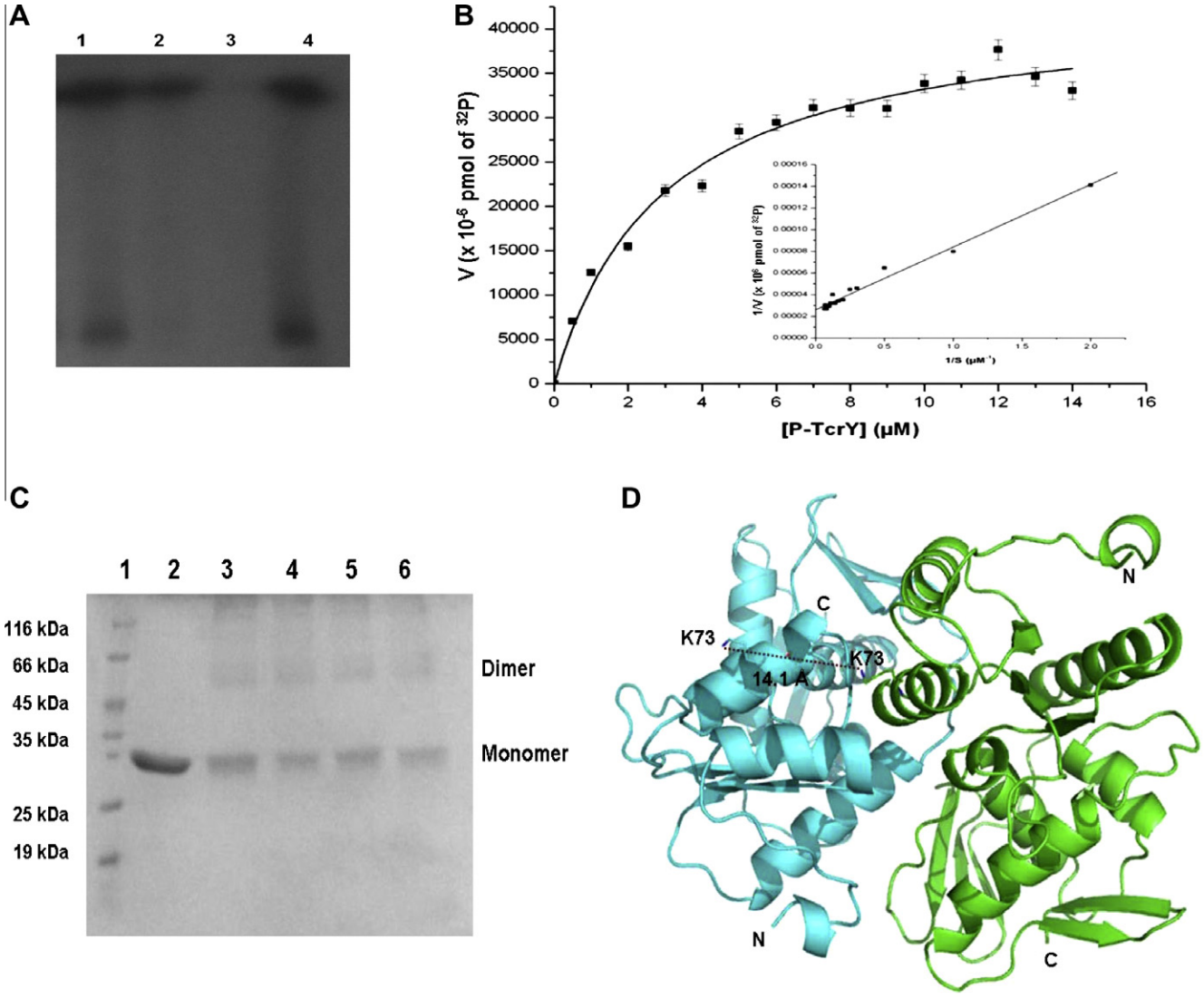

Fig. 1. (A) Radioactive phosphorylation assays. Lane 1, TcrY and TcrX; Lane 2, TcrY and TcrX/D54A; Lane 3, TcrY/H256Q; and Lane 4, TcrY and TcrX/D59A. (B) The initial velocities of phosphotransfer from TcrY to TcrX were plotted against the P-TcrY concentration in Michaelis–Menten and Lineweaver–Burk (inset) models. (C) P-TcrX oligomerization by crosslinking in 12% SDS–PAGE: Lane 1, marker; Lane 2, TcrX; Lane 3, TcrX with 1 mM BS^3; Lane 4, TcrX with 2 mM BS^3; Lane 5, P-TcrX with 1 mM BS^3; and Lane 6, P-TcrX with 2 mM BS^3. (D) TcrX–TcrX interaction model by GRAMM-X.

India), ATP and TcrY for 1, 2, 4, 6, 7, 8 and 9 h at 25 °C under phosphorylation conditions [11]. P-TcrX was subsequently purified by Ni-NTA chromatography. The ^{32}P incorporation into TcrX from P-TcrY was found to be highest after 7 h of phosphotransfer based on quantification by liquid scintillation. TcrX or P-TcrX was dialyzed against 1× PBS, pH 7.4. The crosslinking reaction mixture contained 7 μg of TcrX or P-TcrX (after 7 h of phosphotransfer with labeled ATP) mixed with 1 or 2 mM bis(sulfosuccinimidyl) suberate (BS^3) (SIGMA) for 30 min at 25 °C. The reactions were stopped by adding SDS–PAGE loading buffer, and the samples were heated for 5 min at 95 °C. The proteins were analyzed by 15 % SDS–PAGE.

2.4. In silico TcrX–DNA docking

The dimeric model of TcrX was prepared by the GRAMM-X server [18]. The lowest energy model with lysines at distances near the BS^3 crosslinkable range was selected. The overall architecture was similar to the PrrA dimer (PDB id 1YS6), the closest homolog of TcrX. The template DNA Pm3 (Fig. 2C) was modeled as B-DNA by 3DDART portal [19] of the HADDOCK server using a global modeling mode. The TcrX–DNA interaction models were generated by the HADDOCK server [20]. The models were visualized and analyzed by PyMOL (http://www.pymol.org/) and PDBe PISA [21], respectively.

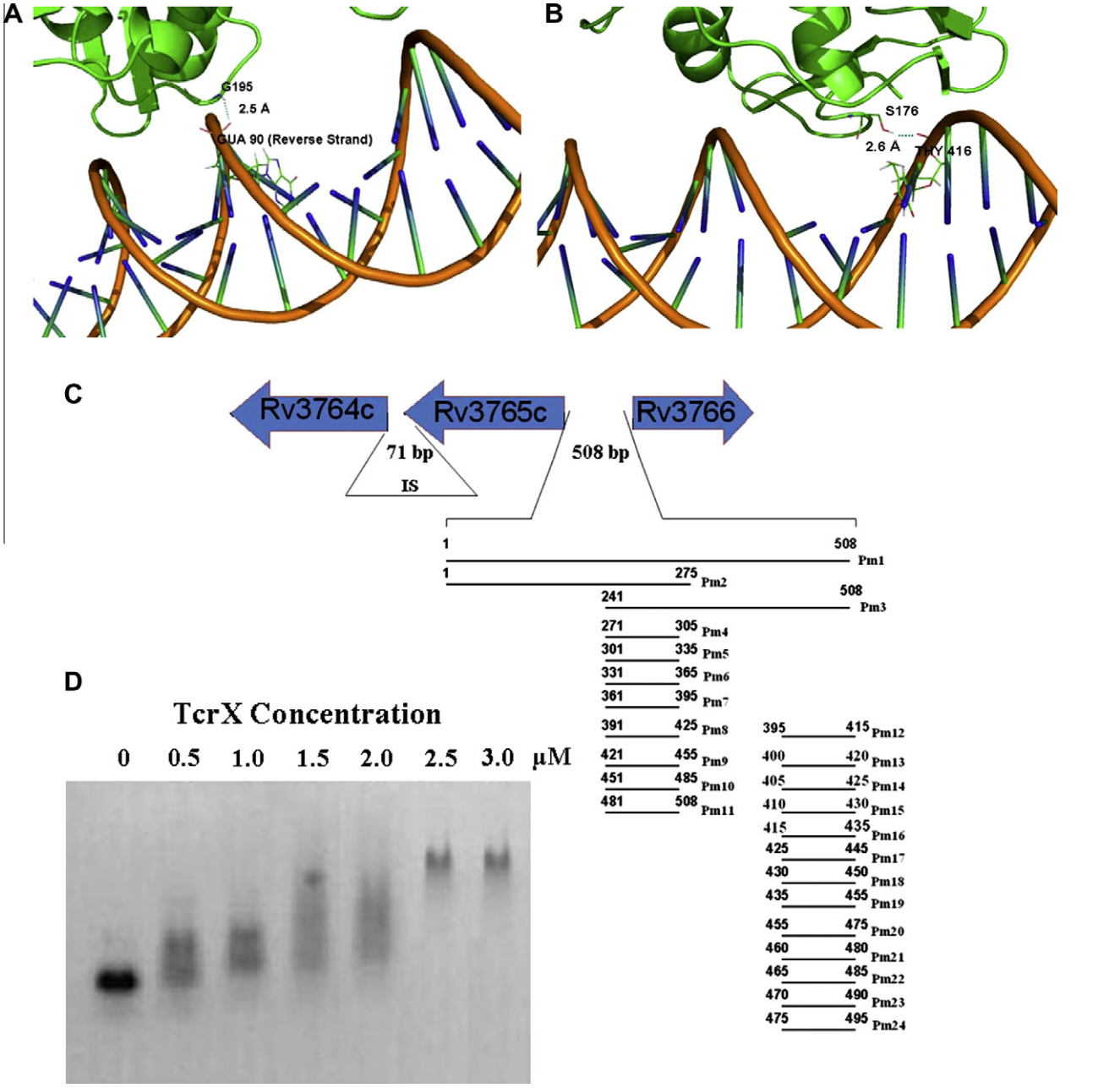

Fig. 2. (A) Interaction between G195 of one TcrX subunit and GUA 90 of the reverse strand complementary to CYT 419, which is in the 412–426 bp region. (B) Interaction between S176 of the other TcrX subunit interacting with THY 416 in the 412–426 bp region. (C) Schematic diagram of the 508-bp promoter region (Pm1) and intergenic sequence (IS) between Rv3764c and Rv3765c. The fragmentation of Pm1 into smaller overlapping segments (Pm2–Pm24). (D) TcrX concentration-dependent EMSA with TcrX concentrations of 0, 0.5, 1.0, 1.5, 2.0, 2.5 and 3.0 μM.

2.5. EMSA

The promoter region (508 bp) representing the intergenic region between ORFs Rv3765c and Rv3766 was amplified by PCR from H37Rv genomic DNA. The smaller fragments were obtained by complementary oligo annealing (Supplementary Tables 2 and 3). P-TcrX was prepared with 10 μCi [γ-^{32}P] ATP in presence of TcrY for 7 h as described in Section 2.3. DNA fragments were labeled with [γ-^{32}P] ATP (>3300 Ci/mmol, BRIT, India) and T4 polynucleotide kinase (Fermentas) and purified by nucleotide removal kit (QIAGEN). Competition assays were performed with the unlabeled specific promoter Pm1 in 0-, 50- and 100-fold molar excess of the labeled promoter. Herring testes DNA were used as a non-specific competitor at 100-fold molar excess of the labeled Pm1 for the competition assays. Concentration-dependent EMSAs were conducted with 0.5–3.0 μM of TcrX. TcrX or P-TcrX (2.5 μM in each case) was incubated with 10 nM of labeled PCR amplified fragments (Pm1–Pm3) or labeled oligo annealed fragments (Pm4–Pm24) in 1× binding buffer (50 mM NaCl, 25 mM Tris–HCl, pH 7.4, 2 mM $MgCl_2$, 1 mM EDTA and 6% v/v glycerol) for 1 h at 25 °C in a reaction volume of 10 μl. The samples were run on 1% TAE agarose gel and subjected to autoradiography.

2.6. Circular dichroism

Circular dichroism (CD) spectra were recorded in the "far-UV" region on a Jasco-J-810 spectropolarimeter with a path length of 0.1 cm. The data points were recorded using step resolution of 0.2 nm, a time constant of 2 s, sensitivity of 10 mdeg, a scan speed of 50 nm/min and a spectral bandwidth of 2.0 nm with four scans per sample. For each CD spectrum, 10 μM TcrX, P-TcrX or TcrX (D54A) in dialysis buffer was used. Each final spectrum was an average of three scans. The protein spectra were collected and subtracted from the buffer spectra.

3. Results and discussion

3.1. TcrX/Y phosphorylation

The conserved residues TcrY/H256 and TcrX/D54/D59 were mutated to analyze their respective roles in the phosphotransfer process. The *in silico* model of the TcrX and TcrY interaction predicted the involvement of TcrY/H256 and TcrX/D54 in phosphorylation [11]. TcrX/D59 was in close proximity to TcrX/D54. However, multiple sequence alignments showed both of the TcrX aspartate residues (D54 and D59) to be conserved [11]. Hence, the exact aspartate involved in His-Asp phosphorylation between TcrY (HK) and TcrX (RR) was probed by site-directed mutagenesis. D54A and D59A mutants of TcrX and the H256Q mutant of TcrY were prepared. The molecular weights of GST tagged TcrY (H256Q) and His_6 tagged TcrX (D54A and D59A) were found to be ~52 and ~30 kDa, respectively, from 15% SDS–PAGE analysis (Fig. S1A and B). In contrast to TcrY, autophosphorylation was not observed with TcrY (H256Q) in the presence of [γ-^{32}P] ATP (Fig. 1A), suggesting that H256 is indispensable for the activity of TcrY. In contrast to TcrX, TcrX (D54A) was not phosphorylated by TcrY, whereas TcrX (D59A) was phosphorylated (Fig. 1A), suggesting that D54 is the site of phosphate acceptance from TcrY. The phosphate transfer kinetics between

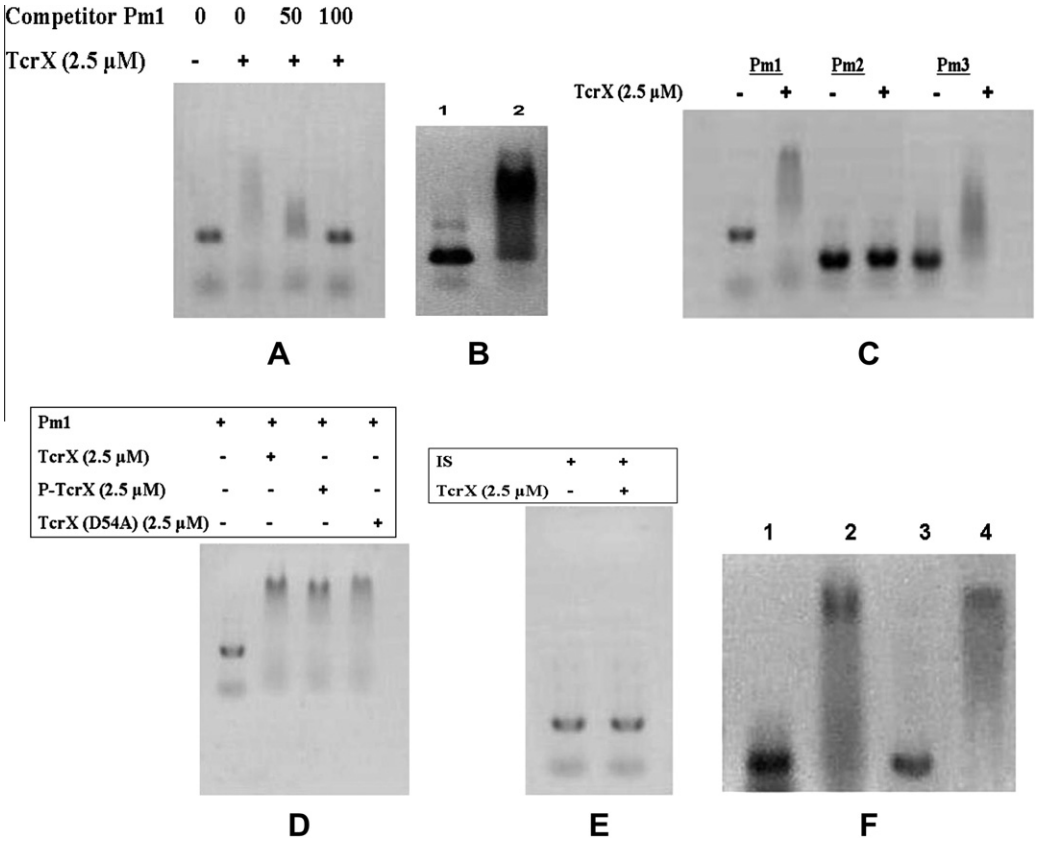

Fig. 3. (A) Competition assay with unlabeled Pm1 added at 0-, 50- and 100-fold molar excess of labeled Pm1. "+" and "−" designates with or without TcrX (2.5 μM), respectively. (B) Competition assay of non-specific herring testes DNA with labeled Pm1 at 100-fold molar excess. Lane 1, labeled Pm1; Lane 2, gel shift of labeled Pm1 with TcrX (2.5 μM) in presence of 100-fold molar excess of herring testes DNA. (C) Mobility shift assay of Pm1, Pm2 and Pm3. "+" and "−" depicts with or without TcrX (2.5 μM), respectively. (D) EMSA of radiolabeled Pm1 with 2.5 μM each of TcrX, P-TcrX, TcrX (D54A). "+" and "−" depicts with or without TcrX, P-TcrX or TcrX (D54A). (E) IS in the presence of 2.5 μM of TcrX. "+" and "−" depicts with or without TcrX (2.5 μM), respectively. (F) EMSA with ^{32}P-TcrX and radiolabeled Pm1. Lane 1, Pm1; Lane 2, gel shifted Pm1 by ^{32}P-TcrX; Lane 3, Pm1; and Lane 4, gel shifted Pm1 by TcrX.

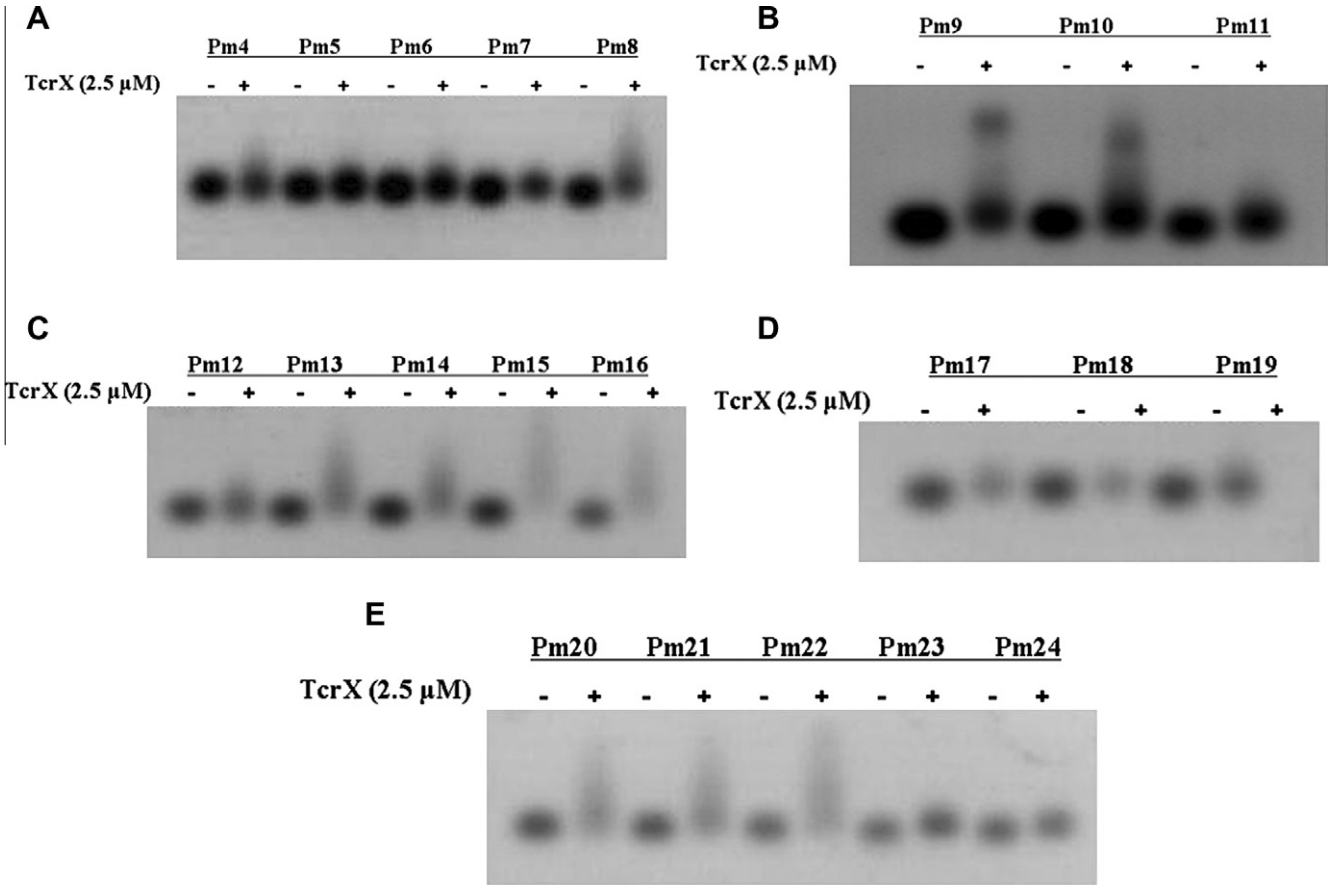

Fig. 4. EMSA with radiolabeled fragments. (A) Pm4–Pm8, (B) Pm9–Pm11, (C) Pm12–16, (D) Pm17–19, and (E) Pm20–24 in presence of 2.5 μM of TcrX. "+" and "−" depicts with or without TcrX (2.5 μM), respectively.

TcrX/Y was determined in presence of [γ-^{32}P] ATP. The transfer of labeled phosphate from TcrY to TcrX was monitored using a scintillation counter. After fitting the initial velocities at different concentrations of P-TcrY in a Michaelis–Menten plot, a K_m value of 3 μM was obtained (Fig. 1B). This is similar to the K_m values of 1.5 μM for KinA/Spo0A and 6.5 μM for CheA/CheY phosphotranfer kinetics [22,23].

3.2. TcrX dimerization by crosslinking

Phosphorylation dependent and independent dimerization of RRs has previously been reported [24,25] and was the motivation behind the study of the dimeric nature of TcrX and P-TcrX. The dimerization of TcrX was analyzed using BS^3 to crosslink amino groups in close proximity within TcrX. Upon crosslinking with BS^3, dimeric TcrX was observed at ~60 kDa (Fig. 1C). P-TcrX dimer concentrations were similar to the TcrX dimer concentrations observed by BS^3 crosslinking, indicating that phosphorylation has no influence on the extent of TcrX dimerization (Fig. 1C). The phosphorylation independent dimerization nature of TcrX is similar to that of PhoP from *Salmonella enterica* [25]. Oligomerization of TcrX is not enhanced by phosphorylation, whereas the fraction of Mycobacterial PhoP in the dimeric state is greatly increased upon phosphorylation [24]. Oligomerization and DNA binding of some RRs, such as Streptococcal CovR, occurs only after phosphorylation [26].

3.3. TcrX-DNA docking

The dimeric model of TcrX obtained from GRAMM-X with crosslinkable lysines (K73) 14 Å apart has a similar architecture to the PrrA dimeric structure from *M. tuberculosis* (Fig. 1D). The interacting interface of the dimeric TcrX is composed of 31 residues and is stabilized by three hydrogen bonds and 18 salt bridges, as obtained from ProtoRP [27]. The TcrX$_{Dimer}$-DNA complex (ΔG = −24.2 kcal/mol) modeled using HADDOCK is much more stable than the TcrX dimer alone (ΔG = −4.4 kcal/mol) (Fig. S2).

The dimer interaction is specifically observed between the winged helix-turn-helix (wHTH) motif of TcrX and the 412–426 bp region of the promoter (Fig. S3A). The wHTH signature motif of RRs is known for recognizing DNA. Residues involved in the TcrX–DNA interaction are shown in Fig. 2A and B. These residues reside in α6–α8 region, with α8 being the recognition helix that is expected to interact with the major groove of the DNA.

3.4. TcrX specifically binds to the tcrX promoter region

The RR-DNA interaction has been found to be autoregulatory in *M. tuberculosis* [28–33]. TcrX bound the labeled *tcrX* promoter Pm1 (Figs. 2C and 3C). The least mobility was observed with the highest concentration (2.5 μM) of TcrX (Fig. 2D). Competition assays with unlabeled specific promoter were performed to verify the specificity of TcrX binding to the *tcrX* promoter. The 50- and 100-fold molar excess of unlabeled Pm1 disrupted the mobility shift of labeled Pm1 (Fig. 3A). The competition assays with unlabeled non-specific herring testes DNA performed in 100-fold molar excess showed that the interaction of TcrX with Pm1 is specific (Fig. 3B). The effect of P-TcrX and TcrX (D54A) on Pm1 binding was also explored because phosphorylation of a RR has its own effect on DNA binding [34,35] (Fig. 3D and F). P-TcrX or TcrX (D54A) showed no change in conformation as measured by Circular Dichroism, suggesting there is no difference in binding activity (Fig. S1D). Thus, the DNA-binding ability of TcrX is independent of its phosphorylation state. TcrX

did not bind to the 71-bp intergenic sequence (IS) between Rv3764c and Rv3765c indicating the absence of *tcrX* promoters within the 71-bp IS (Fig. 3E). EMSAs with various overlapping promoter fragments were conducted to determine the minimal sequence of DNA recognized by TcrX (Fig. 2C). The observation of a positive gel shift with Pm3 led to a more detailed screen of this region (Fig. 3C). Pm3 was fragmented into overlapping shorter fragments (Pm4–Pm11) among which Pm8–Pm10 showed a positive gel shift assay (Figs. 2C and 4A and B). The region encompassing the Pm8–Pm10 fragments was divided into thirteen overlapping fragments of 21 bp each (Pm12–Pm24) (Fig. 2C). Two binding regions were observed (Pm13–Pm16 and Pm20–Pm22) (Fig. 4C and E), which was contrary to our theoretical study that predicted a single binding site (412–426 bp or Pm13–Pm16 region). Inspection of these binding sites revealed an inverted repeat in the 412–426 bp and 455–470 bp regions before the translational start site. The DNA sequence was also analyzed by the Mfold web server [36] for secondary structures formed by the stretches of DNA that encompassed the binding regions. An energetically favorable ($\Delta G = -10.46$ kcal/mol) loop structure is observed near the regulatory sequence (Fig. S3A). The inverted repeats in the loop structure are therefore closer in space than in sequence, which would facilitate the binding of TcrX. The observed diffused protein-DNA banding may be attributed to the fact that active TcrX probably requires approximately 30 bp of DNA for proper DNA binding. Hence, complete gel shifts were obtained with the comparatively larger DNA fragments Pm1 (508 bp), Pm3 (267 bp), Pm9 (35 bp) and Pm10 (35 bp). The smaller DNA fragments Pm13, Pm14, Pm15, Pm16 and Pm20–22 (21 bp each) are unable to show complete gel shifts, resulting in smeared banding patterns. Based on the previous study of strong promoter sequences primarily required for characterization of Mycobacterial promoter regions [37], we have annotated the putative Shine Dalgarno and −10 and −35 boxes of the *tcrX* promoter region (Fig. S3B).

Most of the OmprB/PhoB subfamily members bind to direct repeats except those that bind to inverted repeats, such as PmrA from *S. enterica* [38] and RegX3 from *Mycobacterium smegmatis* [39]. TcrX can be grouped in with subfamily members that bind inverted repeats. The RRs can be divided into four categories based on their preference toward phosphorylation and subsequent DNA binding. Class I RRs represent proteins that bind to their target genes only after phosphorylation, e.g., ArcA [34] and NarL [40], whereas Class II RRs comprise the members that bind target DNA more tightly in the phosphorylated state. Most of the RRs, including OmpR [41] and PhoB [42], belong to Class II. Class III comprises the RRs that can bind to DNA equally in the unphosphorylated and phosphorylated form, as observed with PhoP from *M. tuberculosis* and *S. enterica* [24,33]. The Class IV RRs bind to DNA in their unphosphorylated form and phosphorylation decreases their DNA-binding ability, e.g., CsgD from *Salmonella typhimurium* [43]. TcrX from *M. tuberculosis* belongs to Class III because it can bind to its target DNA sequence in the unphosphorylated state and phosphorylation does not enhance DNA binding.

Acknowledgments

We acknowledge DST and DBT, GOI for funding. We thank Prof. Y. Zhang, JHSPH for H37Rv genomic DNA, IICB, for liquid scintillation analyzer facility. Prof. A.K. Ghosh, IIT Kharagpur is acknowledged for his suggestion. We also thank Dr. Somnath Mukherjee and Mr. Debajyoti Dutta for helpful discussions.

Appendix A. Supplementary data

Supplementary data associated with this article can be found, in the online version, at doi:10.1016/j.bbrc.2011.09.143.

References

[1] J.A. Hoch, T.J. Silhavy, Two-component Signal Transduction, Am. Soc. Microbiol., Washington, DC, 1995.
[2] A.M. Stock, V.L. Robinson, P.N. Goudreau, Two-component signal transduction, Ann. Rev. Biochem. 69 (2000) 183–215.
[3] I. Smith, *Mycobacterium tuberculosis* pathogenesis and molecular determinants of virulence, Clin. Microbiol. Rev. 16 (2003) 463–496.
[4] S.B. Walters, E. Dubnau, I. Kolesnikova, F. Laval, M. Daffe, I. Smith, The *Mycobacterium tuberculosis* PhoPR two-component system regulates genes essential for virulence and complex lipid biosynthesis, Mol. Microbiol. 60 (2006) 312–330.
[5] T.C. Zahrt, V. Deretic, *Mycobacterium tuberculosis* signal transduction system required for persistent infections, Proc. Natl. Acad. Sci. USA 98 (2001) 12706–12711.
[6] D.R. Sherman, M. Voskuil, D. Schnappinger, R. Liao, M.I. Harrell, G.K. Schoolnik, Regulation of the *Mycobacterium tuberculosis* hypoxic response gene encoding α-crystallin, Proc. Natl. Acad. Sci. USA 98 (2001) 7534–7539.
[7] J.S. Tyagi, D. Sharma, Signal transduction systems of mycobacteria with special reference to *M. tuberculosis*, Curr. Sci. 86 (2004) 93–102.
[8] J. Bacon, L.G. Dover, K.A. Hatch, Y. Zhang, J.M. Gomes, et al., Lipid composition and transcriptional response of *Mycobacterium tuberculosis* grown under iron limitation in continuous culture: identification of a novel wax ester, Microbiology 153 (2007) 1435–1444.
[9] S.E. Haydel, J.E. Clark-Curtiss, Global expression analysis of two-component system regulator genes during *Mycobacterium tuberculosis* growth in human macrophages, FEMS Microbiol. Lett. 236 (2004) 341–347.
[10] T. Parish, D.A. Smith, S. Kendall, N. Casali, G.J. Bancroft, N.G. Stoker, Deletion of two-component regulatory systems increases the virulence of *Mycobacterium tuberculosis*, Infect. Immun. 71 (2003) 1134–1140.
[11] M. Bhattacharya, A. Biswas, A.K. Das, Interaction analysis of TcrX/Y two component system from *Mycobacterium tuberculosis*, Biochimie 92 (2010) 263–272.
[12] E.M. Hackert, A.M. Stock, Structural relationships in the OmpR family of winged-helix transcription factors, J. Mol. Biol. 269 (1997) 301–312.
[13] T. Yamane, H. Okamura, M. Ikeguchi, Y. Nishimura, A. Kidera, Water-mediated interactions between DNA and PhoB DNA-binding/transactivation domain: NMR-restrained molecular dynamics inexplicit water environment, Proteins 71 (2008) 1970–1983.
[14] I. Baikalov, I. Schroder, M. Kaczor-Grzeskowiak, D. Cascio, R.P. Gunsalus, R.E. Dickerson, NarL dimerization? Suggestive evidence from a new crystal form, Biochemistry 37 (1998) 3665–3676.
[15] A.E. Maris, M. R Sawaya, M. Kaczor-Grzeskowiak, M.R. Jarvis, S.M. Bearson, M.L. Kopka, I. Schroder, R.P. Gunsalus, R.E. Dickerson, Dimerization allows DNA target site recognition by the NarL response regulator, Nat. Struct. Biol. 9 (2002) 771–778.
[16] J.G. Pelton, S. Kustu, D.E. Wemmer, Solution structure of the DNA-binding domain of NtrC with three alanine substitutions, J. Mol. Biol. 292 (1999) 1095–1110.
[17] S.N. Ho, D.H. Henry, R.M. Horton, J.K. Pullen, L.R. Peasea, Site-directed mutagenesis by overlap extension using the polymerase chain reaction, Gene 77 (1989) 51–59.
[18] A. Tovchigrechko, I.A. Vakser, GRAMM-X public web server for protein-protein docking, Nucl. Acids Res. 34 (2006) 310–314.
[19] M. van Dijk, A.M.J.J. Bonvin, 3D-DART: a DNA structure modelling server, Nucl. Acids. Res. 37 (2009) W235–W239.
[20] M. van Dijk, A.D.J. van Dijk, V. Hsu, R. Boelens, A.M.J.J. Bonvin, Information-driven Protein-DNA Docking using HADDOCK: it is a matter of flexibility, Nucl. Acids Res. 34 (2006) 3317–3325.
[21] E. Krissinel, K. Henrick, Inference of macromolecular assemblies from crystalline state, J. Mol. Biol. 372 (2007) 774–797.
[22] Y.L. Tzeng, J.A. Hoch, Molecular recognition in signal transduction: the interaction surfaces of the spo0f response regulator with its cognate phosphorelay proteins revealed by alanine scanning mutagenesis, J. Mol. Biol. 272 (1997) 200–212.
[23] R.C. Stewart, Kinetic characterization of phosphotransfer between CheA and CheY in the bacterial chemotaxis signal transduction pathway, Biochemistry 36 (1997) 2030–2040.
[24] A. Sinha, S. Gupta, S. Bhutani, A. Pathak, D. Sarkar, PhoP–PhoP interaction at adjacent PhoP binding sites is influenced by protein phosphorylation, J. Bacteriol. 190 (2008) 1317–1328.
[25] P.P. Savard, G.D. Crescenzo, H.L. Moual, Dimerization and DNA binding of the *Salmonella enterica* PhoP response regulator are phosphorylation independent, Microbiology 151 (2005) 3979–3987.
[26] A.A. Gusa, J. Gao, V. Stringer, G. Churchward, J.R. Scott, Phosphorylation of the group A Streptococcal CovR response regulator causes dimerization and promoter-specific recruitment by RNA polymerase, J. Bacteriol. 188 (2006) 4620–4626.
[27] C. Reynolds, D. Damerell, S. Jones, ProtorP: a protein-protein interaction analysis server, Bioinformatics 25 (2009) 413–414.
[28] S. Himpens, C. Locht, P. Supply, Molecular characterization of the mycobacterial SenX3–RegX3 two-component system: evidence for autoregulation, Microbiology 146 (2000) 3091–3098.

[29] S.E. Haydel, W.H. Benjamin Jr, N.E. Dunlap, J.E. Clark-Curtiss, Expression, autoregulation, and DNA binding properties of the *Mycobacterium tuberculosis* TrcR response regulator, J. Bacteriol. 184 (2002) 2192–2203.
[30] F. Ewann, C. Locht, P. Supply, Intracellular autoregulation of the *Mycobacterium tuberculosis* PrrA response regulator, Microbiology 150 (2004) 241–246.
[31] G. Bagchi, S. Chauhan, D. Sharma, J.S. Tyagi, Transcription and autoregulation of the *Rv3134c-devR–devS* operon of *Mycobacterium tuberculosis*, Microbiology 151 (2005) 4045–4053.
[32] H. He, T.C. Zahrt, Identification and characterization of a regulatory sequence recognized by *Mycobacterium tuberculosis* persistence regulator MprA, J. Bacteriol. 187 (2005) 202–212.
[33] S. Gupta, A. Sinha, D. Sarkar, Transcriptional autoregulation of *Mycobacterium tuberculosis* PhoP involves recognition of novel direct repeat sequences in the regulatory region of the promoter, FEBS Lett. 580 (2006) 5328–5338.
[34] Y. Jeon, Y.S. Lee, J.S. Han, J.B. Kim, D.S. Hwang, Multimerization of phosphorylated and non-phosphorylated ArcA is necessary for the response regulator function of the Arc two-component signal transduction system, J. Biol. Chem. 276 (2001) 40873–40879.
[35] R.G. Brennan, The winged-helix DNA-binding motif: another helix-turn-helix takeoff, Cell 74 (1993) 773–776.
[36] M. Zuker, Mfold web server for nucleic acid folding and hybridization prediction, Nucl. Acid Res. 31 (2003) 3406–3415.
[37] N. Agarwal, A.K. Tyagi, Mycobacterial transcriptional signals: requirements for recognition by RNA polymerase and optimal transcriptional activity, Nucl. Acid. Res. 15 (2006) 4245–4257.
[38] M. Marc, S.M. Wösten, E.A. Groisman, Molecular characterization of the PmrA regulon, J. Biol. Chem. 274 (1999) 27185–27190.
[39] R.T. Glover, J. Kriakov, S.J. Garforth, A.D. Baughn, W.R. Jacobs Jr, The two-component regulatory system *senX3–regX3* regulates phosphate-dependent gene expression in *Mycobacterium smegmatis*, J. Bacteriol. 189 (2007) 5495–5503.
[40] M.S. Walker, J.A. DeMoss, NarL-phosphate must bind to multiple upstream sites to activate transcription from the *narG* promoter of *Escherichia coli*, Mol. Microbiol. 14 (1994) 633–641.
[41] C.G. Head, A. Tardy, L.J. Kenney, Relative binding affinities of OmpR and OmpR-phosphate at the *ompF* and *ompC* regulatory sites, J. Mol. Biol. 281 (1998) 857–870.
[42] D.W. Ellison, W.R. McCleary, The unphosphorylated receiver domain of PhoB silences the activity of its output domain, J. Bacteriol. 182 (2000) 6592–6597.
[43] K. Zakikhany, C.R. Harrington, M. Nimtz, J.C.D. Hinton, U. Römling, Unphosphorylated CsgD controls biofilm formation in *Salmonella enterica* serovar Typhimurium, Mol. Microbiol. 77 (2010) 771–786.